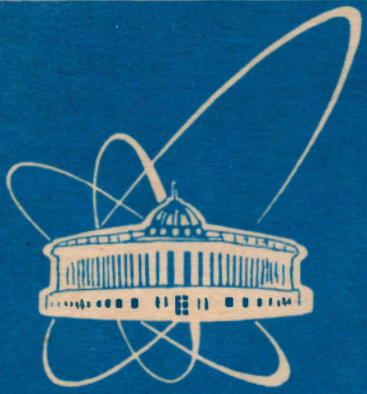

ОБЪЕДИНЕННЫЙ
ИНСТИТУТ
ЯДЕРНЫХ
ИССЛЕДОВАНИЙ

Дубна

E13-95-547

V.V.Karpukhin, I.V.Kisel, A.S.Korenchenko,
S.M.Korenchenko, N.P.Kravchuk, N.A.Kuchinsky,
S.Ritt[1], N.V.Khomutov

CYLINDRICAL MULTIWIRE PROPORTIONAL CHAMBERS FOR THE **PIBETA** DETECTOR OF RARE PION DECAYS

Submitted to «Nuclear Instruments and Methods»

[1]University of Virginia, USA. Now at Paul Scherrer Institut, Villigen, Switzerland

1995

1 Introduction

The spectrometer PIBETA is being developed now at PSI (Switzerland) for experimental investigations of rare pion and muon decays. A goal of this experiment at the first stage is to improve the accuracy of measuring the probability of the pion beta decay from 4% to 0.5%.

Precise measurement of the pion β-decay probability at this level makes it possible to rigorously verify the universality of the charged quark-lepton current and the unitarity of the Cabbibo-Kobayashi-Maskawa mixing matrix [1, 2].

It is planed to perform the experiment at the PSI meson factory in a π^+-beam of momentum ~ 100 MeV/c with stopping intensity up to $5 \cdot 10^6 \pi^+/sec$.

The experimental setup is shown schematically in Fig. 1.

Pions which have traveled through the beam counters are stopped and decay in the active target. The target is surrounded by two cylindrical multiwire proportional chambers (CMPC) to detect charged particles. A cylindrical hodoscope is placed outside the chambers. It consists of high time resolution scintillation counters. All this is surrounded by the shower calorimeter made of pure CsI crystals detecting gamma quanta from π^0-meson decay. The total solid angle for detection of the setup is $\sim 0.77 \cdot 4\pi$ steradian.

The cylindrical proportional chambers are intended for measurement of the charged-particle coordinates with an accuracy ≤ 0.5 mm and ensure a high degree of suppression of the false coincidences of positrons from muon decay. The total amount of matter in the radial cross section of the chambers should be made as small as possible. This is important for successful detection of positrons with low energies, and also for decreasing the probability of gamma conversion into electron-positron pairs in the matter of the chambers.

2 Design and parameters of CMPC

A general description of the design and operation of CMPC can be found in [3]. The chambers are independent self-supporting two-coordinate ones. The azimuthal coordinate is determined by the numbers of the triggered wires located along the cylinder axis. The event coordinate along the cylinder axis is determined from analysis of the induced signals on a cathode split up into separate strips.

Table 1 contains the basic parameters of the chambers. The cross section of the chambers is shown in Fig. 2.

The anode wires are stretched between the flanges connected to a thin-walled supporting lavsan cylinder. The cathode strips are placed on the inner (respective to the anode) surface of the lavsan cylinder. The helical strips on the inner and outer cathode cylinders are curled in opposite directions. The

Table 1: Basic parameters of the CMPC.

Chamber	*CMPC-1*	*CMPC-2*
Active chamber length (mm)	350	540
Total chamber length (mm)	580	730
Diameter of anode (mm)	120	240
Number of anode wires	192	384
Anode wire distance (mm)	1.96	1.96
Anode-cathode gap (mm)	2.5	2.5
Resistance of anode wires (Ω)	110	155
Number of strips at the inner surface	2×64	192
Slope angle of strips at the inner surface (°)	36.96	44.60
Number of strips at the outer surface	2×64	192
Slope angle of strips at the outer surface (°)	-33.65	-42.34
Width of the cathode strips (mm)	3	2.4
Distance between strips (mm)	0.4	0.3

slope angles of strips to the base of the cylinder are listed in Table 1.

The inner cathode cylinder is combined with a supporting cylinder, and the outer protective cathode cylinder is used as a cover to keep the gas inside. The required accuracy and stability of the cathodes and supporting cylinder is ensured by assembling them of several specially cut lavsan film layers glued together.

The anode is made of gold-plated $W(Re)$ wires (3% Re) of diameter 20 μm.

The tension of the wires measured after the initial deformation of the supporting cylinder is 44–48 g for CMPC-1 and 44–51 g for CMPC-2. This tension is sufficient to ensure stable operation despite deformation caused by ageing and possible variations of temperature and humidity. The supporting cylinders were tested under double stress.

In the CMPC-1 the strips make more than one full turn around the cathode cylinder, therefore each strip is split in two halves to avoid an ambiguity in determining the axial coordinate and to increase a rate capability of the chamber. The signals are fed to amplifiers from the both ends of the chamber.

The strips of the PIBETA chamber are made of aluminum foil (thickness < 6 μm) and are connected to connectors by welded wires. This new technology provides much more reliable work of cathodes (especially at high intensity beams) because they are less subjected to electrochemical and gas discharge erosion.

The main geometrical parameters of the chambers are implemented with an accuracy of ± 0.1 mm.

A detailed description of the chamber design (for CMPC-1 as an example) is given in [5]. The materials with low atomic numbers are mainly used for the chambers. This allows to make "transparent" chambers with the total amount of matter in a working region of the order of 10^{-3} radiation lengths.

The data on the matter in the chambers are given in Table 2.

Table 2: Data on the matter in the chambers.

		Radius	Material	Dimensions	Amount of matter	
		mm		mm	mg$\times$ cm^{-2}	rad.len. $\times 10^{-3}$
C	Support. cylinder	57.25	Lavsan	thickness 0.26	36.14	0.906
M	Inner cathode	57.5	Aluminum	3×0.006(step 3,4)	1.43	0.060
P	Anode	60.0	Tungsten	ϕ 0.02 (step 2,0)	0.30	0.045
C	Outer cathode	62.5	Aluminum	3×0.006 (step 3,4)	1.43	0.060
	Protect. cylinder	62.5	Lavsan	thickness 0.105	14.60	0.366
1	Total:				53.90	1.442
C	Support. cylinder	117.2	Lavsan	thickness 0.31	43.09	1.080
M	Inner cathode	117.5	Aluminum	2.4×0.006(step 2.7)	1.44	0.060
P	Anode	120.0	Tungsten	ϕ 0.02 (step 2.0)	0.30	0.045
C	Outer cathode	122.5	Aluminum	$2,4 \times 0.006$(step 2.7)	1.44	0.060
	Protect. cylinder	122.5	Lavsan	thickness 0.205	28.49	0.714
2	Total:				74.76	1.959

Positive high voltage is supplied to the CMPC anode wires. The chamber wires are combined into groups of 32 wires. All the wires in each group are connected to each other by resistors of 0.5 MΩ. The high voltage is fed through a resistor of 20 MΩ to the first and the last wires in each group. Such arrangement of the wire groups allows independent setting (or changing) the high voltage for different zones of a chamber. The signals from the anode wires are read out via the high-voltage blocking capacitors of 500 pF. All the cathode strips are connected to the ground through resistors of 0.8 MΩ, so the cathode surfaces have a zero potential.

3 Chamber test

The test set-up is shown schematically in Fig. 3. A collimated electron beam from a ^{90}Sr source crosses both chambers and hits a scintillation counter. Each group of the anode wires crossed by the beam gave out a fast OR signal. The

trigger signal for the chamber readout system was formed by coincidences of the fast OR signals from CMPC-2 (or CMPC-1) and signals from the scintillation counter when CMPC-1 (or CMPC-2) was respectively studied.

For the anode readout we used the electronics which had been developed at JINR for the experiment to search for muonium-antimuonium transition at PSI.

The cathode signals from the strips were amplified by the current amplifier CSA-32 (current gain 500±2%, noise 3300 e^-) and fed to the analogue-to-digital converters (ADC) via 200 ns delay coaxial cables.

We used the standard LeCroy 1882F ADC. Amplifiers CSA-32 were specially developed for the PIBETA experiment.The method of measurement was describedin [5].

The design of the PIBETA setup does not allow the anode and cathode amplifiers to be placed immediately on the chambers. Therefore the signals from the chambers are transmitted via the coaxial cables (a wave resistance of the cable is 50 Ω, length is 1.5 m).

During the tests the chambers operate using a mixture of gases: 49.9% argon, 49.9% ethane, and 0.2% freon ($CBrF_3$) at atmospheric pressure with continuous flushing.

In Fig. 4 are shown the efficiency of the anode wires (for the discriminator threshold 2 μA) and the leakage currents in the chambers as a function of high voltage applied to the chamber. The efficiency curve for CMPC-1 is shifted in comparison with CMPC-2 to ≈ 50 V because of anode-cathode gap variations (in the admittance limits ±0.1 mm)

The main contribution to the leakage currents is not connected with the electrical processes in gas and does not affect the working characteristics of the chambers. A component of the current linearly rising with the rise in the high voltage is caused by the value constant at the volume and surface resistance of the camber flanges.

Typical distributions of the cathode signal induced on the cathode strips for events when only one wire is hit are shown in Fig. 5. The average number of triggered strips is 4 in CMPC-1 and 5 in CMPC-2.

The cathode surface is taken into account if it contains strips with an amplitude greater than the noise level plus $3.5\sigma_{noise}$.

The efficiencies of the inner and outer strip cathodes as well as the anode wire efficiencies for the discriminator thresholds of 1, 1.5 and 2 μA as functions of high voltage applied to the chamber (CMPC-2) are shown in Fig. 6. For the discriminator threshold of 2 μA the curves for the cathodes and anodes practically coincide.

Similar results were obtained for the CMPC-1 too [5].

From testing data (Figs. 4 and 6) we set the working voltages for CMPC-1

2.35 kV, for CMPC-2 2.45 kV and the discriminator threshold of the anode electronics 2.0 μA.

Fig. 7 shows the distribution of the total charges induced on the inner (Q_{in}) and outer (Q_{out}) cathodes of CMPC-2, and Fig. 8 shows the charge ratio Q_{in}/Q_{out}. The fact that these values are correlated (by large fluctuations) allows one to use the information about strip signal amplitude to avoid an ambiguity in determining the coordinates of multi-track events.

Let us consider a question of coordinate precision in more detail. A charged particle passing through a multiwire proportional chamber near an anode wire (or a group of wires) produces an electron-ion avalanche. The center of gravity of the charge induced on the cathode strips coincides with the coordinates ϕ and Z of the avalanche. In a general case, when the track crosses an anode wire plane at an arbitrary angle, the coordinates ϕ and Z of the crossing point are not the same as the coordinates of the point where the first avalanche started.

The accuracy of determination of the coordinate ϕ of the crossing point is limited by a distance between anode wires S and equals $\sigma = S/\sqrt{12}$.

Further we will consider the case when particles pass normally to the anode wire plane. In this case the Z coordinate of the point where the track crosses the anode wire plane practically coincides with the coordinate of the point where the first avalanche started. A principal limitation to the coordinate determination accuracy along anode wires is connected with the path length of the primary electrones and their diffusion when moving to the place where an avalanche is formed.

Experimental accuracies of the chambers along the Z axis were determined by an indirect method. It is known that the region where an avalanche is formed has maximum dimensions about the size of an anode wire and therefore the centers of the induced charges on the cathodes are located along the anode wires.

Projection on ϕ of the reconstructed centers of the induced charges for the case of single wire hits of chamber CMPC-2 is shown in Fig. 9. Individual wires are clearly visible.

The center of the induced cathode signal is defined as a center of intensity corrected to compensate the systematic errors caused by the discrete structure of the cathode strips [6, 7].

The distribution width ($\sigma' \approx 0.2$ mm) can be considered as an accuracy of wire position determination. The accuracy of the avalanche position along the Z axis can be obtained from the formula:

$$\sigma'_z \approx \tan\left(\frac{\alpha_1 + \alpha_2}{2}\right)\sigma' < \sigma',$$

where α_1 and α_2 are the absolute values of the strip slope angles on the inner and outer surfaces.

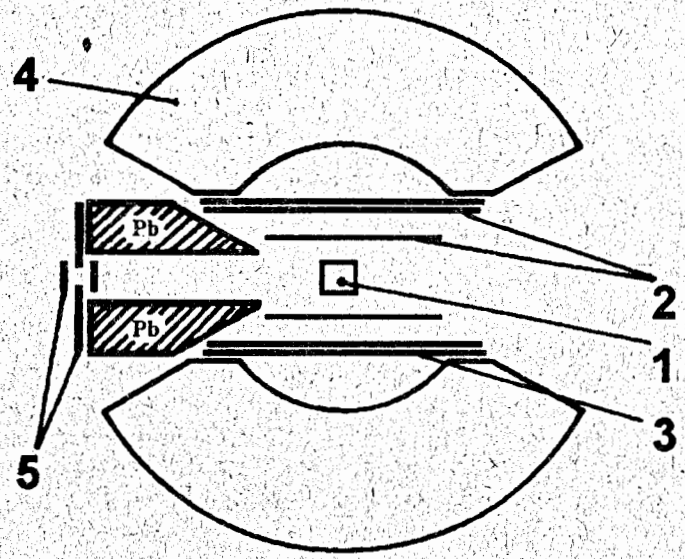

Fig. 1: Schematic depiction of the experimental setup PIBETA: 1 – active target; 2 – CMPCs; 3 – scintillation counters; 4 – sphere of 240 CsI crystals; 5 – beam counters.

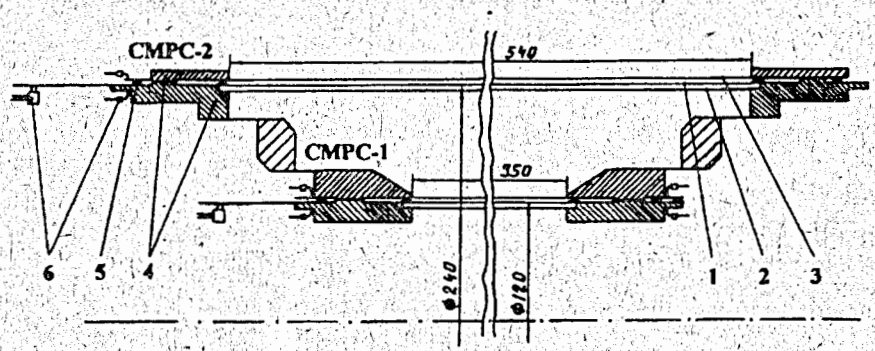

Fig. 2: Sectional view of complete CMPCs (the axis of rotation is at the bottom horizontally): 1 – anode wires; 2 – supporting cylinder and inner cathode; 3 – protective cylinder and outer cathode; 4 – chamber flanges; 5 – gas gasket; 6 – anode wires and cathode stripes read out and sockets for wires and strips.

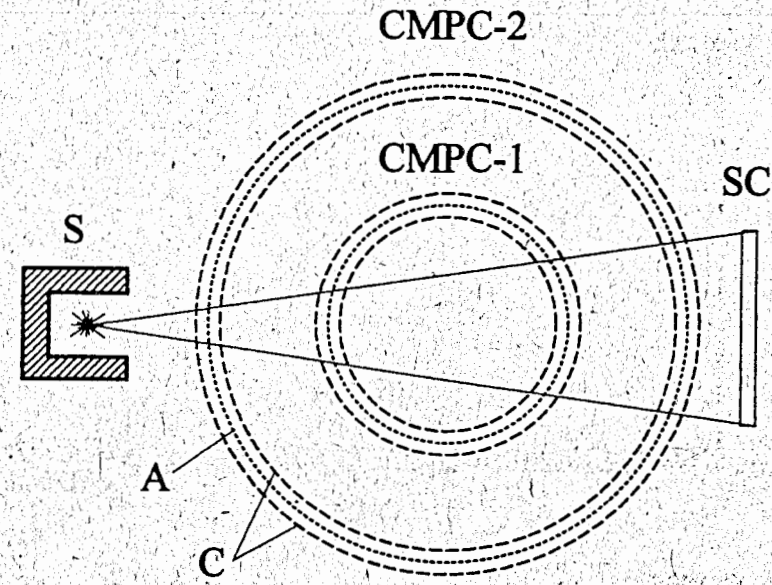

Fig. 3: The test run set-up: S – ^{90}Sr source; SC – scintillation counter; A – anode wires of the CMPC; C – cathode strips of the CMPC.)

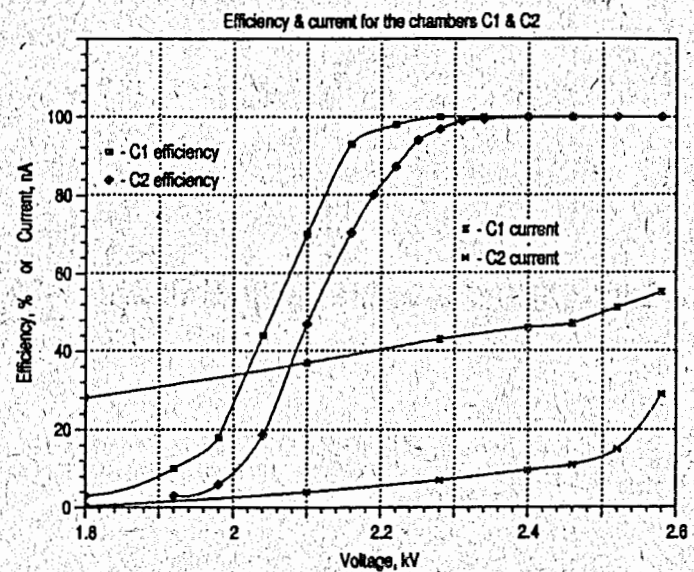

Fig. 4: Efficiency of the anode wires and the leakage currents in the chambers.

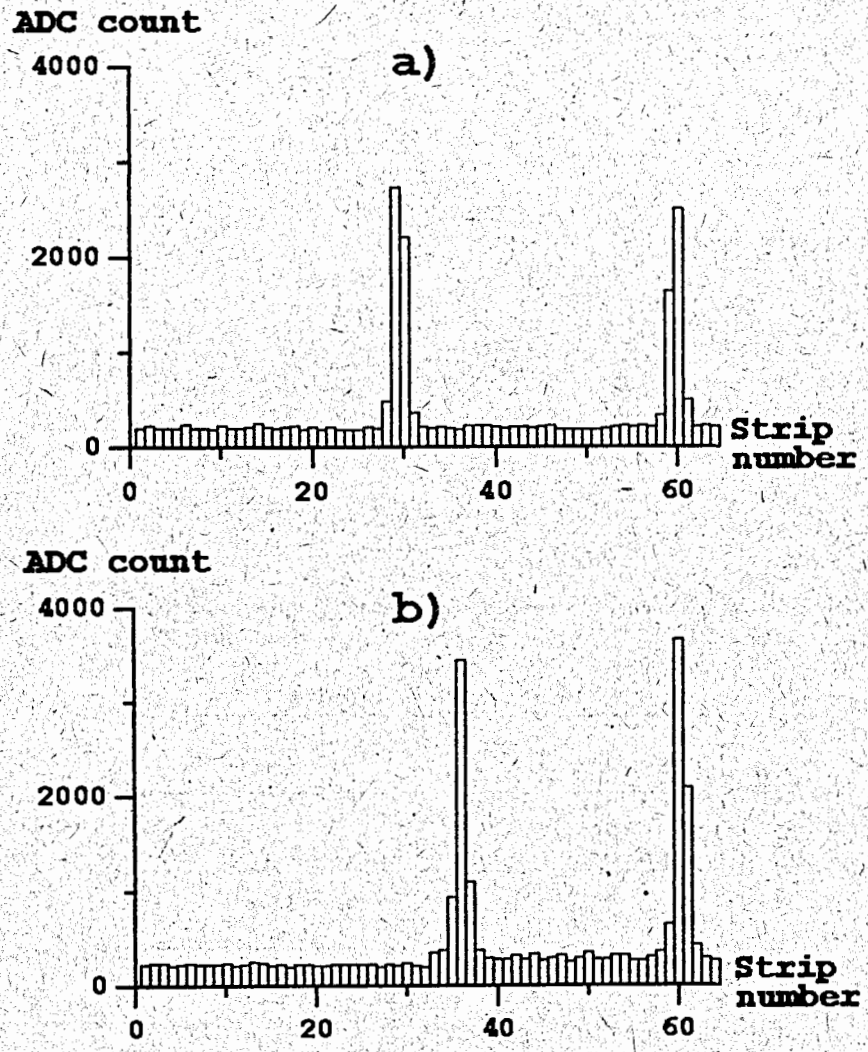

Fig. 5: Distributions of the signals induced on the cathode strips: a) inner surface, b) outer surface

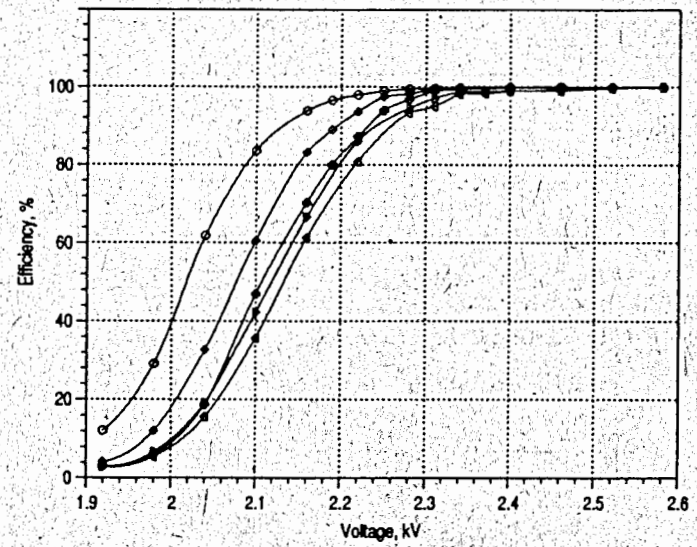

Fig. 6: Anode wire efficiency for different discrimination thresholds (⊙ — 1 μA, ◇ 1.5 μA, + 2 μA) and cathode strip efficiency (▷ — inner cathodes, ◁ — outer cathodes).

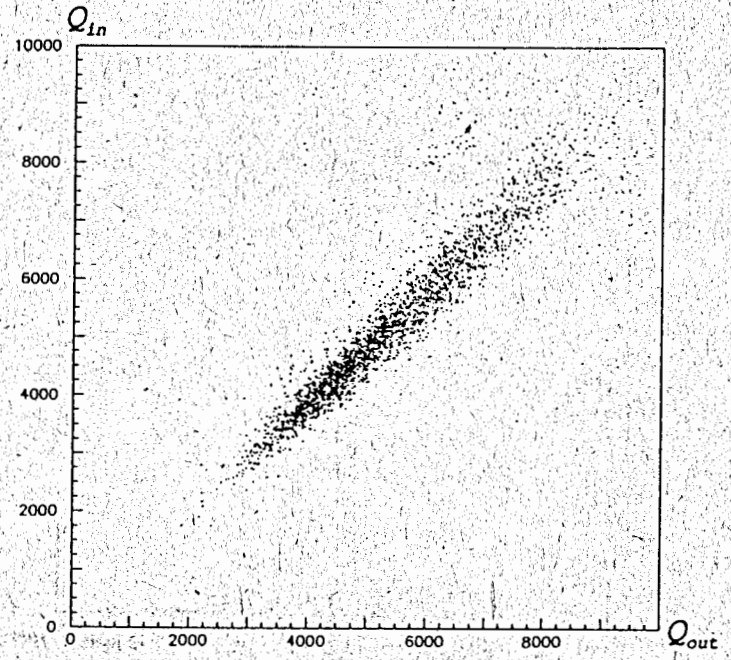

Fig. 7: The scatter plot of the measured charges Q_{in} and Q_{out}.

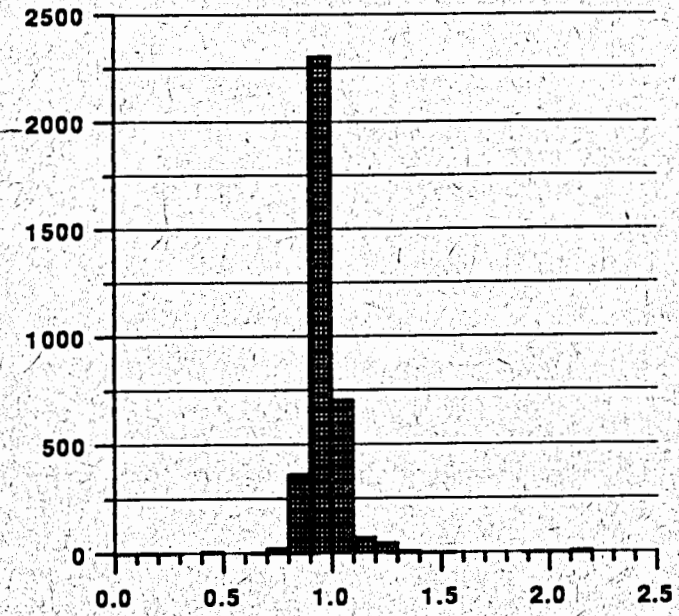

Fig. 8: Example of the correlation between the total charges induced on the inner and outer cathode planes.

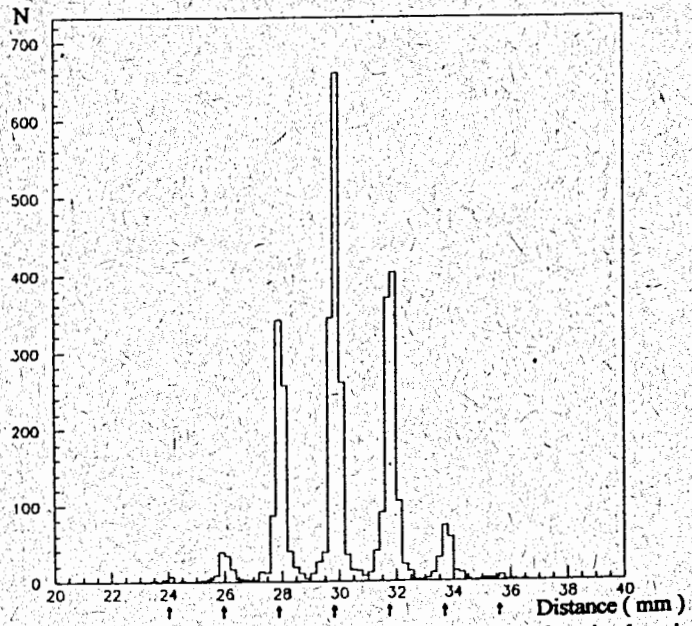

Fig. 9: Centers of induced charges in the ϕ projection for single wire hit. The arrows show wire positions.

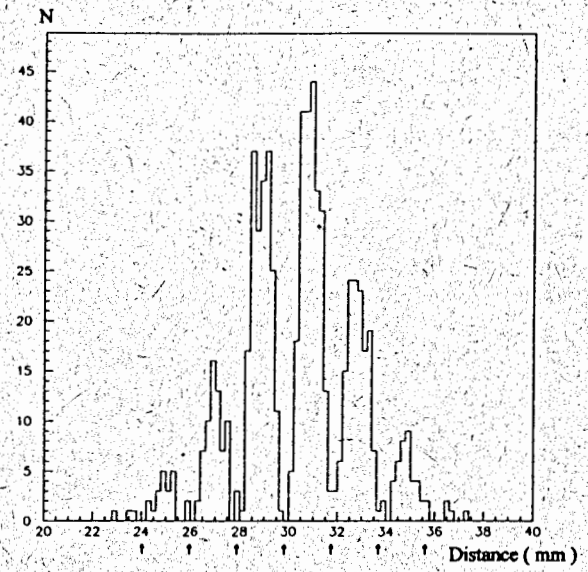

Fig. 10: Centers of induced charges in the ϕ projection for double wire hit clusters. The arrows show wire positions.

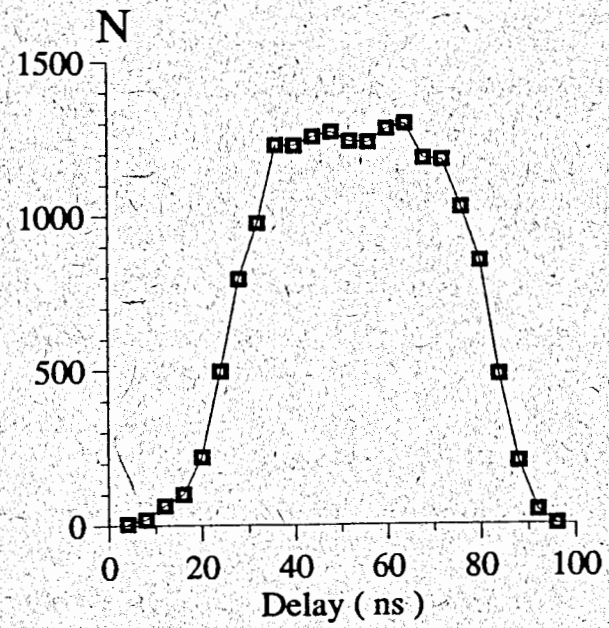

Fig. 11: Delayed coincidences between the anode signal and the strobe pulse.

This is true for the case of an avalanche on a single wire. The two wires hitting probability at the working high voltage is $\sim 25\%$, therefore this case has to be carefully considered. A probability of 3 (or more) wire clusters is less than 1%.

Fig. 10 demonstrates the distribution of the coordinate ϕ of the intersection of centers of gravity of signals induced on two neighbouring wires. The distribution width ($\sigma'' \approx 0.5$ mm) is greater in comparison to Fig. 9 mainly because of different values of cathode signals (Fig. 7) induced from different wires. It causes additional inaccuracy of Z coordinate determination.

The spatial resolution errors result from statistical nature of ionization processes, electronic noise, data analysis method. In a real experimental situation we have to add errors of mechanical tolerancies of anodes and cathodes and errors caused by the non-zero crossing angle. As a result the reconstruction accuracy can be lowered not more than by ~ 0.2 mm.

The time resolution of the chambers can be estimated from the left slope length (40–50 nsec) of a delayed coincidence curve between the anode signal and the strobe pulse (Fig. 11). The time resolution of the chambers is ~ 25 nsec.

This work is supported by the Russian Foundation for Basic Research and by the INTAS fund.

References

[1] *D. Pocanic, K.A. Assamagan, D. Day et al.* Proposal for an Experiment at PSI, R 89-01.1, 1991.

[2] *K.A. Assamagan, Yu. Bagaturia, V.A. Baranov et al.* Annual report 1993. - PSI Nuclear and Particle Physics Newsletter 1993 Annex I., Villigen: PSI, 1993, p. 35–36.

[3] *N.P. Kravchuk.* Physics of Particles and Nuclei, 1994, 25(5), 1244.

[4] *J. Vanko, N.P. Kravchuk, K.G. Nekrasov, A.I. Filippov, A.P. Fursov.* JINR Communications 13-88-468, Dubna, 1988.

[5] *V.V. Karpukhin, A.S. Korenchenko, S.M. Korenchenko et al.* JINR Preprint 13-95-92, Dubna, 1995.

[6] *A.A. Glazov, I.V. Kisel, G.A. Ososkov.* JINR Communications E10-93-123, Dubna, 1993.

[7] *C. Grab.* A Search for the Decay $\mu^+ \to e^+e^+e^-$, Dissertation, Universität Zürich, 1985.

Received by Publishing Department
on December 29, 1995.

Карпухин В.В. и др. E13-95-547
Цилиндрические пропорциональные камеры
для детектора редких распадов пионов PIBETA

Описывается конструкция и характеристики двухкоординатных цилиндрических многопроволочных пропорциональных камер, изготовленных в ОИЯИ (Дубна) для эксперимента по изучению распада $\pi^+ \to \pi^0 e^+ \nu_e$. Камеры диаметром 120 и 240 мм и длиной 350 и 580 мм выполнены в виде самоподдерживающихся конструкций, содержащих малое количество вещества в радиальном сечении. Координатная информация получается в результате обработки сигналов с анодных проволочек и стрипов. Стрипы размещены на внутреннем и внешнем катодных цилиндрах под углом к проволочкам. Приводятся результаты испытания камер.

Работа выполнена в Лаборатории ядерных проблем ОИЯИ.

Препринт Объединенного института ядерных исследований. Дубна, 1995

Karpukhin V.V. et al. E13-95-547
Cylindrical Multiwire Proportional Chambers
for the PIBETA Detector of Rare Pion Decays

Design and characteristics of two-coordinate cylindrical multiwire proportional chambers manufactured in JINR (Dubna) for experimental investigation of the $\pi^+ \to \pi^0 e^+ \nu_e$ decay are described. The chambers have diameters of 120 and 24 mm, lengths of 350 and 580 mm. The chambers are made as self-supporting constructions containing small amount of matter in radial cross section. Information about the coordinates is obtained after processing of the signals from anode wires and strips. The strips are placed on inner and outer cylinders at an angle to the wires. The results of the chamber test are given.

The investigation has been performed at the Laboratory of Nuclear Problems, JINR.

Preprint of the Joint Institute for Nuclear Research. Dubna, 1995